Environ Geol (2009) 57:1457–1467
DOI 10.1007/s00254-008-1423-9

ORIGINAL ARTICLE

Geochemical distribution and removal of As, Fe, Mn and Al in a surface water system affected by acid mine drainage at a coalfield in Southwestern China

Pan Wu · Changyuan Tang · Congqiang Liu · Lijun Zhu · TingQuan Pei · Lijuan Feng

Received: 25 September 2007 / Accepted: 9 June 2008 / Published online: 17 July 2008

Abstract The chemical characteristics, formation and natural attenuation of pollutants in the coal acid mine drainage (AMD) at Xingren coalfield, Southwest China, are discussed in this paper based on the results of a geochemical investigation as well as geological and hydrogeological background information. The chemical composition of the AMD is controlled by the dissolution of sulfide minerals in the coal seam, the initial composition of the groundwater and the water–rock interaction. The AMD is characterized by high sulfate concentrations, high levels of dissolved metals (Fe, Al, Mn, etc.) and low pH values. Ca^{2+} and SO_4^{2-} are the dominant cation and anion in the AMD, respectively, while Ca^{2+} and HCO_3^- are present at significant levels in background water and surface water after the drainage leaves the mine site. The pH and alkalinity increase asymptotically with the distance along the flow path, while concentrations of sulfate, ferrous iron, aluminum and manganese are typically controlled by the deposition of secondary minerals. Low concentrations of As and other pollutants in the surface waters of the Xingren coalfield could be due to relatively low quantities being released from coal seams, to adsorption and coprecipitation on secondary minerals in stream sediments, and to dilution by unpolluted surface recharge. Although As is not the most serious water quality problem in the Xingren region at present, it is still a potential environmental problem.

Keywords Acid mine drainage (AMD) · Hydrogeochemical characteristic · Heavy metals · Natural attenuation · Xingren coalfield

Electronic supplementary material The online version of this article (doi:10.1007/s00254-008-1423-9) contains supplementary material, which is available to authorized users.

P. Wu (✉) · L. Zhu · T. Pei · L. Feng
Key Laboratory of Karst Environment and Geohazard Prevention, Guizhou University, Ministry of Education, Caijiaguan, Guiyang, Guizhou 550003, China
e-mail: pwu@gzu.edu.cn

P. Wu · C. Tang
Faculty of Horticulture, Chiba University, Matsudo, Chiba 271-8510, Japan

C. Liu
State Key Laboratory of Environment, Geochemistry Institute of Geochemistry, Chinese Academy of Sciences, Guiyang 550002, China

Introduction

Guizhou has been known as "home of coal in south China," with a reserve of 241.9 billion tons of coal, some of which contains high levels of As. This coal has been available to the public for many years (Zhou et al. 1993; Ding et al. 1999, 2000), and has even been randomly excavated by local residents. The As-rich coal is used in open stoves without chimneys for cooking, heating and drying corn and hot peppers. Arsenicosis has therefore become an endemic disease in these areas, spreading to five counties in Guizhou (Zhou et al. 1993; Zheng et al. 1999). Although high-As coal seams are only present in these areas, and their exploitation has been forbidden by the local government, acid mine drainage (AMD) and metal leaching have been particular concerns because they will continue indefinitely, causing environmental damage long after the mining operation has ended.

There are generally sulfide minerals such as pyrite (FeS_2) in the coal. Coal mining operations expose pyrite to oxygen

and water, resulting in a series of oxidation and hydrolysis reactions which produce sulfuric acid (e.g., Lowson 1982; Evangelou 1995). This acidity can, in turn, promote the solubilization of heavy metal contaminants which then appear in excessive concentrations in water bodies downstream of the mining activities. The AMD contains high concentrations of cations such as Fe^{3+}, Fe^{2+}, Mn^{2+}, Al^{3+} and anions like SO_4^{2-}, in addition to elements like Cu, Hg, Pb, Zn and As at trace concentrations. Consequently, this degrades the water quality of the region (e.g., Tiwary 2001).

The oxidation mechanisms of sulfide minerals in coal-mining areas have been well described in numerous studies (e.g., Lowson 1982; Evangelou 1995; Allen et al. 1996; Foos 1997; Schuring et al. 1997; Black and Craw 2001; Devasahayam 2006), although the process of sulfide oxidation is complex and generally includes a number of reactants and products. The quality of mine drainage can be controlled by numerous chemical, physical, hydrological, geological, geochemical and biological factors. The metal pollutant concentrations can be attenuated to background levels without any treatment (Bowell and Bruce 1995; Berger et al. 2000; Fukushi et al. 2003), due to the fact that the reaction of AMD with carbonate and/or silicate rocks, and the consequent attainment of a relatively high pH, not only decreases the oxidation rate of sulfides but also reduces the concentrations of several dissolved metals, chiefly through precipitation and sorption (e.g., Holmström et al. 1999; Accornero et al. 2005). An understanding of the main hydrogeochemical mechanisms governing pollutant transfer is therefore required in order to predict and control pollution as well as to implement decontamination procedures (Bodénan et al. 2004). However, there are still gaps in our knowledge of the chemical evolution of AMD and how to control the pollutants in mine drainage under various geological and environmental conditions.

In order to study the behaviors of relevant metals in both water and sediments affected by AMD in a karst-dominated basin, the coalfield in Xingren county, southwestern China, was investigated. The objectives of this study were: (1) to characterize the geochemistry of the mine drainage in the coalfield; (2) to explain the chemical evolution of AMD, which controls the levels of dissolved metals such as Fe, Mn, Al and As; (3) to identify the reactions governing the natural attenuation process.

Location and geology

The Xingren coalfield is one of the important coal districts of China and is located in the Xingren county of Guizhou province, Southwest China (E: 105°00′–105°19′, N: 25°24′–25°35′) (Fig. 1). The region has a subtropical warm–moist climate, with an annual average temperature of 15.2 °C and a relatively high average annual precipitation of 1320.5 mm. About 84% of the annual precipitation falls during May to October.

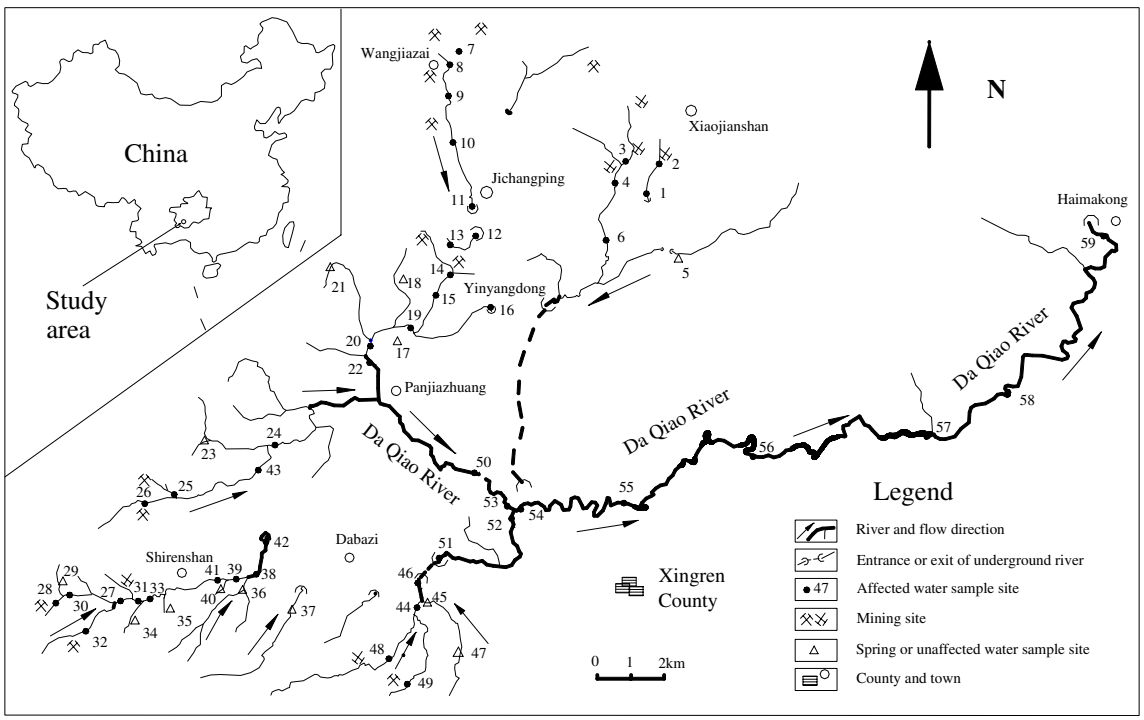

Fig. 1 Location map of the sampling sites in the study area comprising the Xingren coalfield, Southwestern China

The bedrock of the area is mainly composed of sedimentary carbonate rocks from the Permian–Triassic period. They include karstified gray dolomites, dolomitic limestones and gray limestones, sometimes with the occurrence of marls and clays. The coal-bearing strata are mainly hosted in the Permian Longtan Formation, and are characterized by significant differences in number (8–32) and thickness. Up to six coal layers are utilized for a total thickness of about 12 m. Arsenic concentrations are up to 405–7,930 μg/g in several strata in the study area (Ding et al. 1999), and its occurrence in coal seams makes Xingren a typical high-As coalfield in China (Ding et al. 1999, 2000; Zhao et al. 2003; Li et al. 2003). Mudstones, silt-mudstones and siltstones are generally present at the top of the coal layers, while their bottoms consist of clay stones and silt-clay stones. The coal utilized is anthracite with a low–middle ash content, a middle–high sulfur concentration and a high calorific value. Coal mining operations are mainly carried out upstream of the Da Qiao River, such as at Xiaojianshan, Panjiazhuang, Wangjiazai, Shirenshan, and so on (Fig. 1). More than 25 companies are currently engaged in the exploitation of raw coal, and it was estimated that the total output of raw coal was about 2.5–3.0 million tons every year in Xingren County.

The dominance of jointed and fractured carbonate rocks (both limestone and dolomite) has resulted in the occurrence of karst caves, and karstification is a common feature of the study area. The Da Qiao River is the major river in the study area, with an annual average discharge of 3.9×10^5 m^3/d. There are also several small streams, some of which are underground, that discharge into the Da Qiao River; this river becomes a subterranean stream near Haimakou in the east of the study area (Fig. 1). There are also innumerable abandoned coal mines upstream of the Da Qiao River. The drainage runoff from abandoned or active coal mines flows onto the surface of the wadi and infiltrates the mainstream and branches of the Da Qiao River.

Methodology

Surface water and groundwater (spring and cave water) in the Xingren coalfield were sampled in April 2005. In order to expediently discuss the chemical characteristics, formation and natural attenuation of the pollutants in the coal mine drainage, the water types were classified into two groups based on both their hydrodynamic relationships and geological conditions. In general, the waters receiving the coal mine drainage are termed "affected waters," while background waters (including spring water, cave water and surface water) that are not polluted by the coal mine drainage are called "unaffected waters" in the following discussion. All of the representative water samples were collected using the grab technique, and the sampling site locations are shown in Fig. 1. Twenty-two sediment samples were also collected in the vicinity of the coal mines, upstream of the Da Qiao River. At each sample site, 1 kg sediment samples were collected with a homemade core sampler at a depth of 0–5 cm, placed into a plastic bag, and then transported to the laboratory.

Temperature, pH, electrical conductivity and dissolved oxygen were measured, and all of the water samples were filtered through 0.45 μm filters on-site. Alkalinity was also determined by acidimetric titration in the field. All samples were collected in high-density polyethylene bottles and were stored in a refrigerator at 4°C before laboratory analyses. Filtered, unacidified samples were used for the determination of major anions by ion chromatography (IC, ICS-90, Dionex Corp., Sunnyvale, CA, USA). The sulfate concentration in some samples was also determined gravimetrically by adding saturated $BaCl_2$ solution to form $BaSO_4$ precipitate. The filtrates were acidified to $pH < 2$ with reagent-grade HNO_3 to avoid Fe hydroxide precipitation, and were analyzed for major cations by inductively coupled plasma spectrometry. Major elements (Na, Mg, Ca, K, Fe, Al, and Mn) were analyzed by ICP-OES (Vista MPX, Varian, Palo Alto, CA, USA), and As was analyzed by ICP-MS (Platform ICP) in the State Key Laboratory of Environment Geochemistry, Institute of Geochemistry, Chinese Academy of Sciences. Blanks and appropriate certified reference standards were analyzed as unknowns with every batch of samples. The ion balance was computed to check for possible errors in the analysis of major components, and the charge unbalance was found to be <10% in most cases and <15% in few cases.

The total As concentration in sediments was analyzed by atomic fluorescence spectrometry (AFS-230E) after extraction and treatment with antiscorbutic acid and thiourea (Xie et al. 2006). The geochemical computer code PHREEQC, version 2.2 (Parkhurst and Appelo 1999), was used for speciation–saturation calculations.

Results and discussions

General characteristics of the water quality

The statistical parameters for the geochemical variables considered for the collected waters are summarized in Table 1, whereas all of the analytical data are given in "Appendix 1." As shown in Table 1, the waters affected by AMD exhibited a wide range of conductivities (373–4,010 μS/cm) and pH values (from 2.7 to 8.4), and high average contents of SO_4^{2-} (582 mg/L) and total Fe (34.1 mg/L). These variations between sampling points can be explained by the different contributions of AMD, since mine drainage enters the river without any artificial intervention.

Table 1 Statistical data for the geochemical parameters in affected and unaffected surface waters of the Xingren coalfield, Southwestern China

Parameter	Affected water (45)					Unaffected water (14)				
	Minimum	Maximum	Average	Median	SD	Minimum	Maximum	Average	Median	SD
T	13.2	29.4	18.5	17.6	3.53	14.6	27.7	18.4	17.7	3.48
DO	3.25	12.10	7.50	7.61	1.87	2.64	9.21	6.87	7.72	2.16
pH	2.69	8.44	5.22	5.06	2.12	6.77	8.67	7.64	7.70	0.62
EC	373	4,010	1,140	842	757	125	710	330	260	194
K^+	0.88	30.0	4.36	3.29	4.38	0.83	2.26	1.47	1.58	0.44
Na^+	1.21	85.7	20.6	15.6	18.1	2.12	8.47	5.06	4.88	1.93
Ca^{2+}	58.7	362	114	93.7	65.2	27.1	97.4	51.9	45.1	20.7
Mg^{2+}	7.0	120	33.0	26.3	20.6	2.5	28.9	10.6	6.22	8.76
Cl^-	0.27	27.8	4.17	2.08	5.95	0.33	5.49	1.64	1.56	1.22
NO_3^-	0.17	46.3	5.41	2.83	8.92	0.13	19.4	4.80	3.49	4.72
SO_4^{2-}	18.1	3,480	580	460	6,130	2.44	260	70.4	25.9	80.4
HCO_3^-	0	320	82.4	21.0	109	33.6	468.2	166.3	130.4	120
Al	0.01	180	13.4	2.75	31.1	bd	2.45	0.21	0.025	0.65
Fe	0.01	740	34.1	2.65	110	bd	0.09	0.02	0.02	0.02
Mn	bd	19.49	4.22	3.26	4.67	bd	1.91	0.14	0.0014	0.51
As[a]	0.07	1.41	0.50	0.46	0.29	0.04	0.64	0.18	0.07	0.19
TDS	340	4,830	900	650	700	170	640	310	246	160

Ion concentrations and TDS in milligrams per liter, except for As (μg/L); temperature in °C; pH in pH units; *EC* electrical conductivity in μS/cm at 25°C, *SD* standard deviation, *bd* below detection limits; the figure in parentheses after the water type means the number of samples

[a] The As concentration at site 2, where the highest As content was 210 μg/L, is not included in the statistical data

The average EC and TDS values were 1,140 μS/cm and 898 mg/L in affected water, respectively, and were notably higher than those for unaffected spring and surface water, which gave means of 327 μS/cm for EC and 313 mg/L for TDS. The high-conductivity samples were taken near the AMD source.

The chemical composition of the affected water is similar to that observed in previous studies (Allen et al. 1996; Yu 1996; Kim and Chon 2001), with low pH, high SO_4^{2-} and TDS (Fig. 2), as well as high concentrations of several dissolved metals. Sulfate is the most abundant anion, as it represents more than 95% of the total anion concentration in low-pH waters, while HCO_3^- is more significant in unaffected water and polluted water with a high pH (resulting from the dissolution of carbonate rocks).

Major element concentrations, plotted on Piper diagrams for each sampling point (Fig. 3), show significant variations, especially for anion contents. Two end-member compositions, one rich in HCO_3^- and the other rich in SO_4^{2-}, are recognizable in Fig. 3. In affected water, Ca^{2+} and SO_4^{2-} are the dominant cation and anion, respectively (Table 1).

In contrast, the unaffected water is characterized by a Ca–Mg–HCO_3 composition, which is typical of karst areas, as indicated by previous studies of the geochemistry of river waters draining karst-dominated terrains (Han and Liu 2004). Mg^{2+}, K^+ and Na^+ are also important cations in

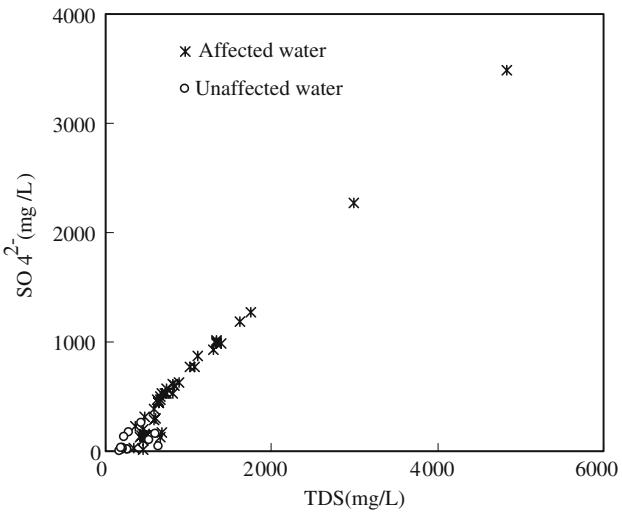

Fig. 2 Correlation plot between dissolved SO_4^{2-} and TDS in the waters of the Xingren coalfield, Southwestern China

affected water, and their contents are higher than those in unaffected water, suggesting that AMD dissolves more clay minerals and carbonate minerals, and consequently yields higher Na^+, K^+, Ca^{2+} and Mg^{2+} concentrations with respect to unaffected water. Although Na^+ and K^+ may derive in part from the dissolution of (K, Na)-bearing minerals, fertilizer pollution is likely to represent an

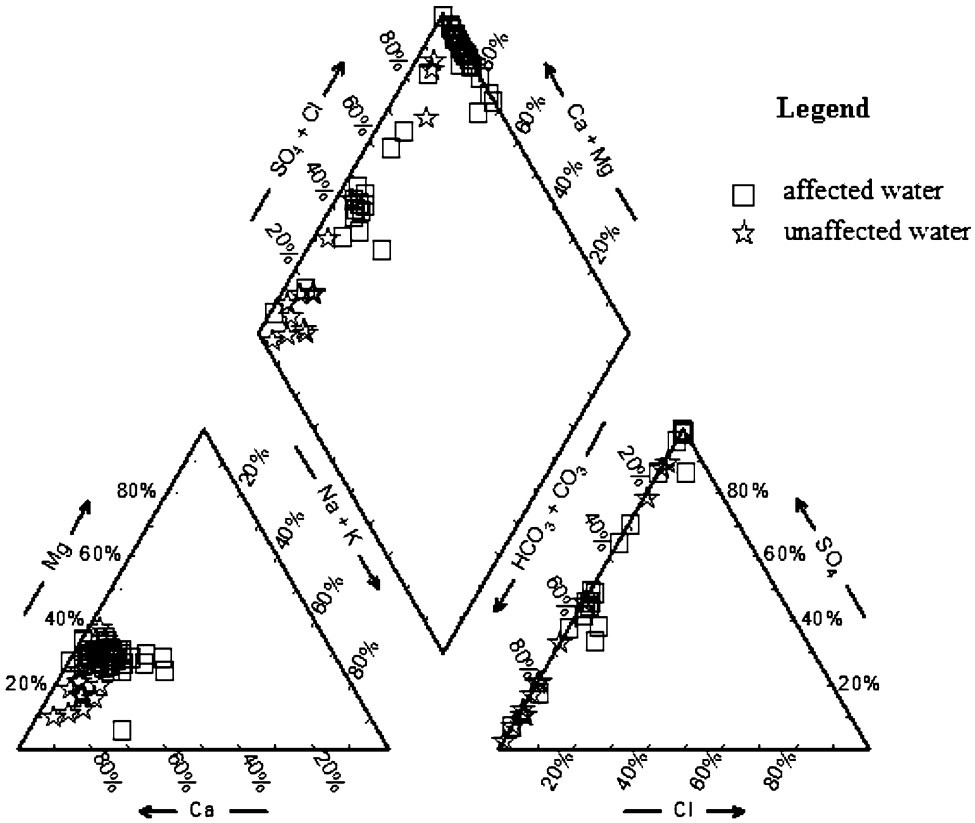

Fig. 3 Piper diagrams for the water samples from the Xingren coalfield, Southwestern China

additional source of alkalis. Other major ion contents vary insignificantly.

Distribution of dissolved metals

The affected waters generally contain significant amounts of easily mobilized dissolved metals. Substantial enrichments in Fe, Al and Mn were detected in affected water, especially close to the mining site. Waters with high total Fe concentrations generally show a relative enrichment in Al and Mn, but there is no strong relationship between measured Fe and Mn (or Al) concentrations in the affected water. Compared with the affected waters, the average contents of the dissolved metals (Fe, Mn, Al) considered are lower for all unaffected waters (Table 1), and even under the detection limits in some samples, suggesting that the dissolution of minerals that potentially release these elements to the aqueous phase proceeds to a very limited extent along the hydrological circuit of unaffected waters. In other words, total Fe, Al and Mn in the studied samples originate mainly from coal mine drainage.

The arsenic level varied widely for affected waters, from 0.06 to 210 μg/L, and over a much smaller interval, from 0.04 to 0.64 μg/L, for unaffected waters (Table 1). Although concentrations of As in the affected waters are highly variable, there is a tendency for some of the relatively high concentrations to occur close to mining areas (Fig. 4). While sample site 2 gave a maximum As concentration of 210 μg/L, most of the As concentrations in the studied samples are much lower—less than 1.00 μg/L. At site 1, which is situated downstream of site 2 at a distance of about 1 km, the As concentration decreases to 0.83 μg/L, suggesting that dissolved As is rapidly removed from waters.

At low pH values, Al sometimes shows conservative behavior, although Al concentrations at a pH of less than ~4.6 and high sulfate concentrations are generally limited by saturation with respect to Al–sulfate–(hydroxyl) solid phases, such as jurbanite, alunite, and alunogen, whereas above pH 4.6 the less soluble phases of gibbsite and/or basaluminite govern Al solubility (Nordstrom 1982). The plot of log Al^{3+} activity versus pH shows that Al^{3+} activity decreases sharply at pH >5, when solid $Al(OH)_3$ begins to form (Fig. 5), consistent with the previous findings of Nordstrom and Ball (1986), as well as those of Berger et al. (2000) and Lee et al. (2002), who interpreted the natural Al precipitates formed in AMD as being amorphous to poorly crystalline, and the observations of Sánchez-España et al. (2006), who studied the removal of dissolved metals during the oxidation and neutralization of AMD.

Iron can be rapidly removed from the aqueous solution through the formation of precipitates with increasing pH, which is supported by observations of yellowish-red precipitates in the field. Figure 6 shows a plot of the calculated activities of Fe^{3+} ion in sampled waters as a function of pH,

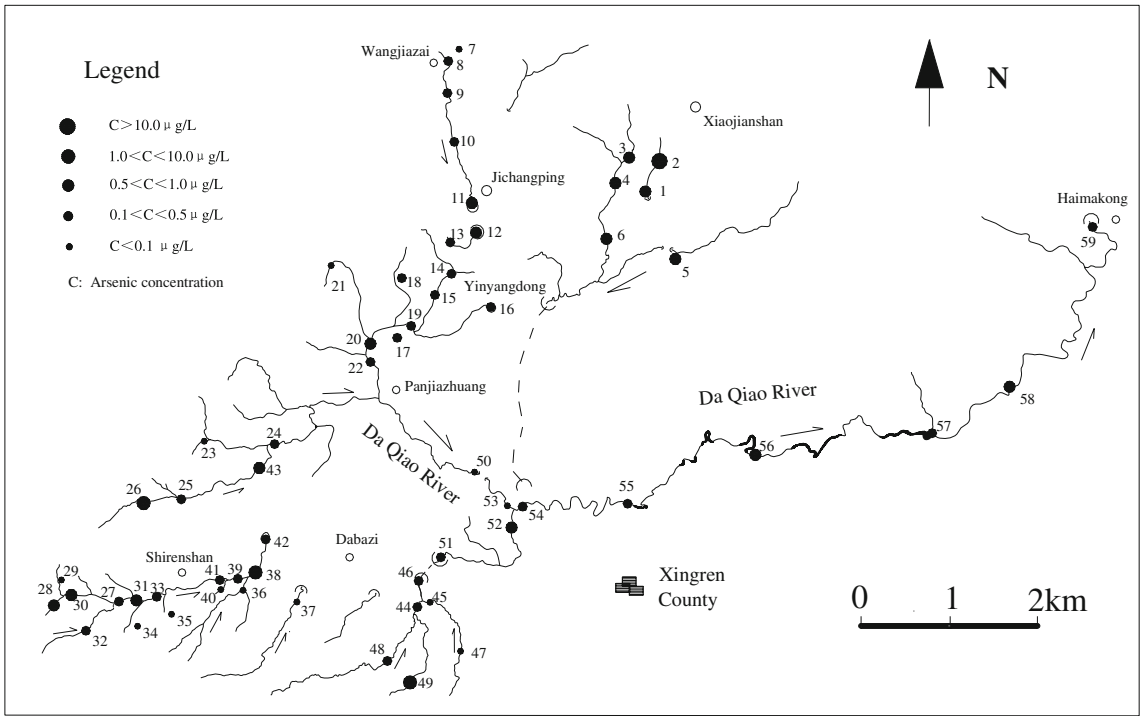

Fig. 4 Arsenic distribution in the waters of the Xingren coalfield, Southwestern China

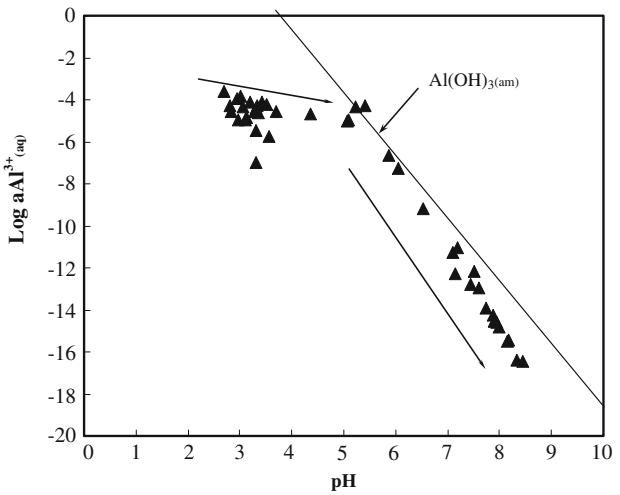

Fig. 5 Plot of log Al^{3+} activities versus pH for the affected waters of the Xingren coalfield. The solubility lines of amorphous $Al(OH)_3$, from Faure (1998) and Lee et al. (2002), are also shown

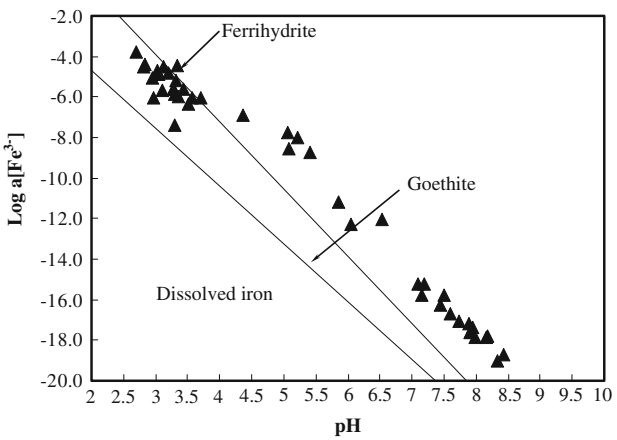

Fig. 6 Plot of the logarithm of Fe^{3+} activity versus pH for the affected waters of the Xingren coalfield. Solubility lines were calculated using the equations of Bigham et al. (1996) for goethite and of Parkhurst (1995) for ferrihydrite

and compares them with the solubility functions of goethite and ferrihydrite. For pH > 4, the data from the study area plot above the solubility line of ferrihydrite, suggesting that the activities of Fe^{3+} ion in these weakly acidic to neutral waters is controlled by the precipitation of Fe(III) oxyhydroxide which is more soluble than species considered in Fig. 6, perhaps corresponding to a ferrihydrite of low crystallinity. Precipitation of schwertmannite may govern the activities of Fe^{3+} ion below pH 4 (see below).

Natural attenuation of pollutants in affected water

AMD can be neutralized by the dissolution of carbonate minerals (Johnson et al. 2000), and even by silicate minerals in some conditions (e.g., Accornero et al. 2005). Although buffering of carbonate dissolution is significant in the study area, mine drainage is initially acidic, because H^+ ions liberated by sulfide oxidation are not immediately consumed by the dissolution of carbonate minerals. Since carbonate rocks are widespread in the study area, when the

mine drainage moves away from the mine sites, the oxidation of sulfide stops, whereas the dissolution of carbonates becomes more and more important, and the acidity previously produced by the oxidative dissolution of pyrite is buffered by carbonate minerals. This is accompanied by a rise in pH values.

Johnson et al. (2000) also underscored the important role played by calcite, even when it is only present in very small amounts (0.1–0.2%), in controlling the pH near neutrality. Although previous studies (e.g., Bodénan et al. 2004; Accornero et al. 2005) show that aluminosilicates can also play a role in some cases, these buffering effects are less important in the short term due to the relatively slow kinetics of aluminosilicate dissolution compared to that of carbonates. Dissolution of carbonate rocks causes an increase not only in pH values but also in Ca^{2+} and Mg^{2+} concentrations. However, Ca^{2+} and Mg^{2+} concentrations gradually decrease during the evolution of mine drainage in the study area. A possible explanation for this is that, along the flow path, cation exchange reactions occur, causing the sorption of Ca^{2+} on the clay fraction and the release of Na^{+}, though simple dilution may also take place. In turn, the removal of Ca^{2+} by ion exchange could cause additional carbonate rocks to dissolve (Mayo et al. 2000).

Pyrite oxidation followed by calcium carbonate buffering may control Ca^{2+} and SO_4^{2-} concentrations in AMD (Ljungberg et al. 1997). The ratio between Ca^{2+} and SO_4^{2-} for the waters from the study area show a clear evolutionary trend (Fig. 7a). Holmström et al. (1999) have proposed the following integrated reaction to describe pyrite oxidation followed by carbonate buffering:

$$FeS_2 + 3.75O_2 + 3.5H_2O + 4CaCO_3 \rightarrow Fe(OH)_3 + 4HCO_3^- + 2SO_4^{2-} + 4Ca^{2+} \quad (1)$$

Equation 1 is consistent with a Ca^{2+}/SO_4^{2-} molar ratio of 2. However, the observed Ca^{2+}/SO_4^{2-} ratios, which are generally less than 1.0 (Fig. 7b), suggest that Eq. 1 is not the only reaction controlling Ca^{2+} and SO_4^{2-} concentrations in the waters of the study area, possibly due to the involvement of Mg-bearing carbonate minerals (e.g., dolomite) in addition to calcite, or other reasons. Saturation indices calculated using PHREEQC indicate that all of the samples are unsaturated with respect to gypsum, in spite of the high SO_4^{2-} and Ca^{2+} concentrations.

The yellowish-red precipitates observed in the field could contain several Fe(III)-bearing secondary minerals. Schwertmannite (ideal formula: $Fe_8O_8(OH)_6SO_4$), a secondary Fe(III) mineral, has been found in mining environments affected by AMD (Bigham 1994; Yu et al. 1999). The precipitation of Fe- and/or Al-bearing solids containing SO_4^{2-} (Bigham et al. 1990) and the adsorption of SO_4^{2-} onto solid surfaces in low-pH aqueous

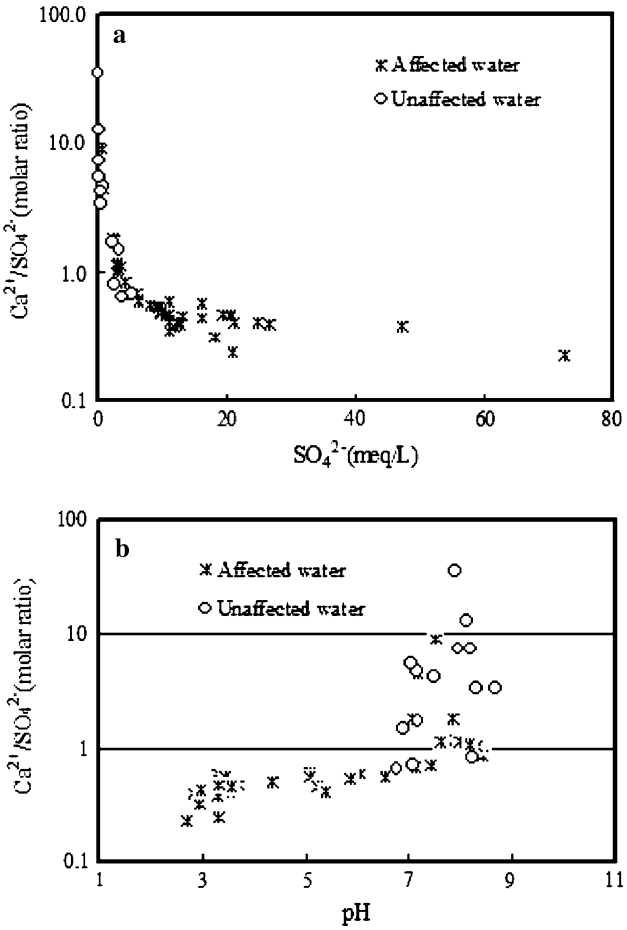

Fig. 7 Ca^{2+}/SO_4^{2-} ratio for the waters of the Xingren coalfield plotted against SO_4^{2-} and pH

environments may be the main mechanisms that cause the decrease in SO_4^{2-} concentration downstream of the affected water. The plot of log SO_4^{2-} activity versus pH (Fig. 8) shows that precipitation of schwertmannite is

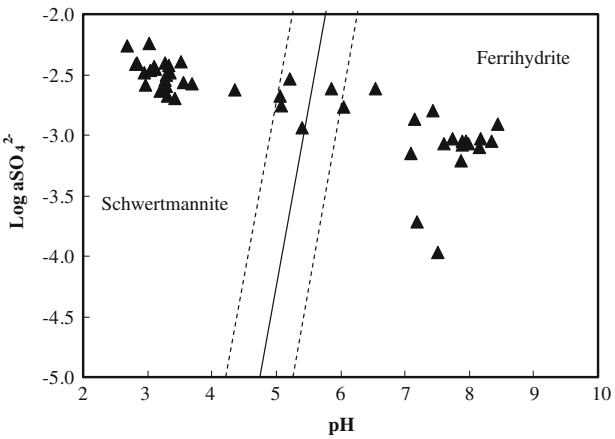

Fig. 8 Plot of the logarithm of SO_4^{2-} activity versus pH for the affected waters of the Xingren coalfield, showing the stability fields of ferrihydrite and schwertmannite

expected to occur at pH < 5.5, whereas ferrihydrite precipitation should take place at pH > 5.5, as suggested by several authors (e.g., Black and Craw 2001; Yu et al. 1999; Williams et al. 2002; Accornero et al. 2005). As shown by these studies, in mine drainage sites, precipitates formed at pH ≥ 6.5 are composed of ferrihydrite or a mixture of ferrihydrite and goethite, whereas those precipitated in the pH range 2.8–4.5 are predominantly composed of schwertmannite with traces of minor amounts of goethite. Lee et al. (2002) reported that Fe is removed from natural waters affected by AMD at pH < 4, Al at pH 5, and Mn at pH 8 during progressive neutralization.

A great many studies on As adsorption on oxides, oxyhydroxides and soils show high adsorption capacities of oxyhydroxides with a maximum around pH 3–5 (Raven et al. 1998; Garcia-Sanchez et al. 2002). The rapid scavenging of As from drainage in an abandoned arsenic mine dump by sorption on hydrous iron oxides was reported by Fukushi et al. (2003). As illustrated in a statistical frequency plot (Fig. 9), the As concentrations in sediments from the study area vary widely, from 20.7 to 219 mg/kg. Sixty-eight percent of samples have As concentrations lower than 60 mg/kg, with an average content of 34 mg/kg.

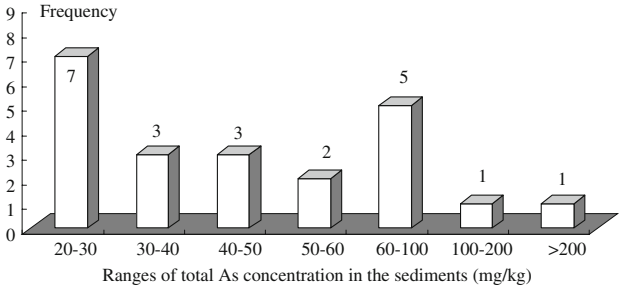

Fig. 9 Frequency plot of arsenic concentration in sediments from streams of the Xingren coalfield, Southwestern China

Although the As concentrations in sediments show large spatial variations, the highest As contents are found close to the discharge of coal mine drainage. Figure 10 shows the spatial distribution of As in the stream sediments at the Xingren coalfield. For example, the As concentrations in sediments are 219 mg/kg at site 2 and 61.8 mg/kg at site 1. These precipitates made up of Fe, Al and Mn oxyhydroxides likely play an important role in the removal of As by adsorption and co-precipitation (Benjaminn 1983; Johnson and Thornton 1987; Stumm and Sulzberger 1992).

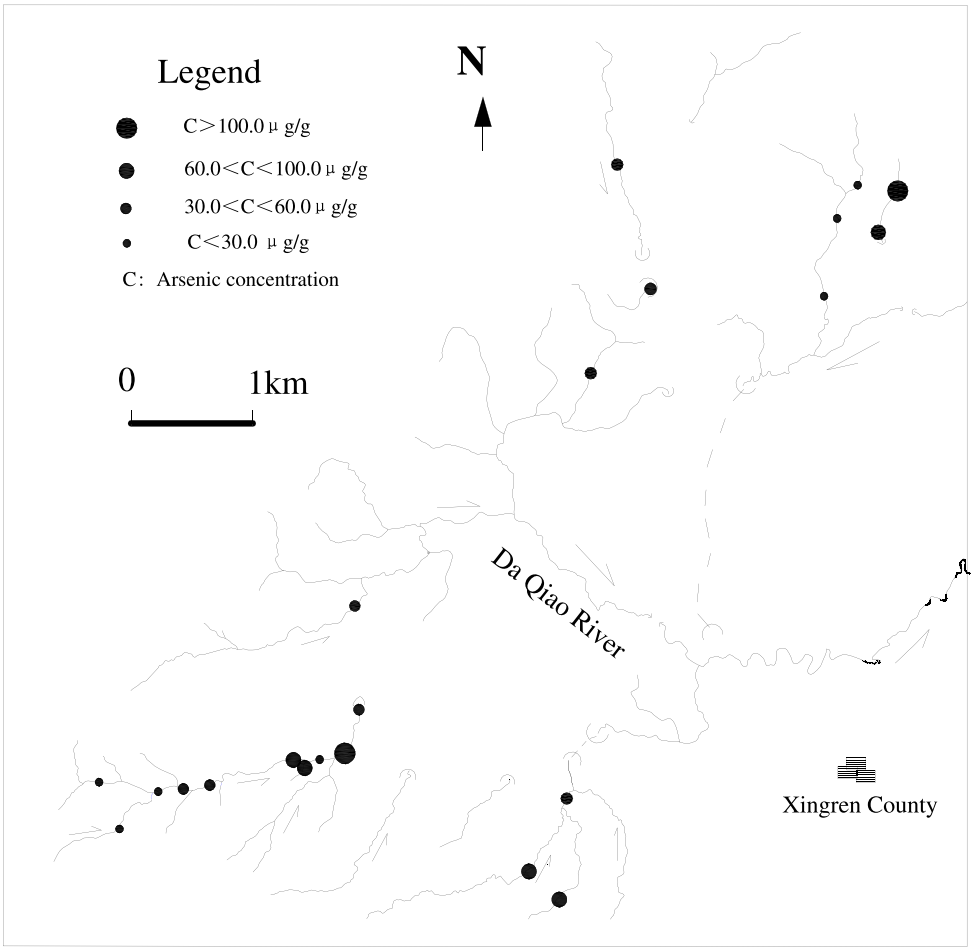

Fig. 10 Arsenic distribution in the sediments of the upper parts of the Xingren coalfield, Southwestern China

Owing to these processes and dilution (addition of unpolluted surface waters), the chemical composition of the affected water downstream of Daqiao River becomes similar to that of background water. Although the evolution of mine drainage may be different from that of background water, the final chemical composition of the affected water becomes similar to that of groundwater through natural attenuation.

Conclusions

The chemical composition of affected waters is controlled by the oxidative dissolution of sulfide minerals in the coal seam, the initial composition of the groundwater and the water–rock interaction. AMD is characterized by high SO_4^{2-} concentrations, high levels of dissolved metals (Fe, Al, Mn, etc.) and low pH values. Ca^{2+} and SO_4^{2-} are the dominant cation and anion in AMD, while Ca^{2+} and HCO_3^- are the prevailing dissolved constituents in background waters.

Owing to the interaction between AMD and carbonate rocks ($CaCO_3$, $CaMg(CO_3)_2$), the pH and alkalinity increase asymptotically with distance along the flow path, while the concentrations of SO_4^{2-}, Fe^{2+}, Al^{3+} and Mn^{2+} are typically attenuated by the deposition of secondary minerals, which results in yellowish-red precipitates being deposited on the stream channel.

Low As concentrations in surface water in the Xingren coalfield could be due to relatively low quantities being released from the coal seam, to As adsorption on secondary minerals in stream sediments, and to dilution by unpolluted surface recharge. Although As is not the most serious water quality problem in the study region at present, it is still a potential environmental problem.

The results of this study also indicate that the concentrations of several dissolved species in AMD-affected water can attain background levels by natural attenuation in this karst-dominated framework.

Acknowledgments We are very grateful to anonymous reviewer(s) for their helpful comments and criticisms of both the English and the scientific writing of the revised manuscript. This project was financially supported by the National Natural Science Foundation of China (40663001; 40463001) and the Governor Special Fund for Outstanding Science and Technology Education of Guizhou Province (2005-119).

Appendix 1

See Table 2.

Table 2 Analytical data for chemical compositions of major ions in affected and unaffected surface waters of the Xingren coalfield, Southwestern China

Sample no.	DO	pH	T	EC	HCO_3	Cl	SO_4	NO_3	K	Na	Ca	Mg	Al	Fe	Mn	As
Affected waters																
1	7.39	3.02	17.5	3,120	0	0.42	2275.18	0.24	2.52	4.33	361.8	115.66	104.27	108.5	19.49	0.833
2	4.20	2.69	16.5	4,010	0	0.27	3483.43	0.73	2.31	2.82	326.48	75.35	180.43	742.05	13.87	210
3	6.36	3.12	19	1,783	0	1.43	985.07	0.37	4.26	22.92	187.77	67.14	5.86	101.66	7.34	0.587
4	5.93	2.84	19.4	2,340	0	1.13	1275.47	0.64	4.90	36.84	210.19	68.34	14.70	139.19	6.81	0.573
6	6.82	2.81	18.7	2,130	0	0.97	1191.56	0.39	4.92	26.52	198.53	69.80	25.26	91.64	8.38	0.559
7	4.15	6.04	14.5	710	75.9	20.99	300.78	46.30	30.03	28.61	73.21	26.71	0.02	0.03	0.01	0.092
8	7.52	3.05	16.7	1,752	0	4.65	926.08	0.17	8.07	60.31	183.53	58.25	19.63	36.34	7.87	0.465
9	7.83	3.28	17.6	1,584	0	3.08	984.32	0.66	5.22	53.24	193.76	57.34	12.66	9.54	6.70	0.485
10	8.08	3.35	17.2	1,468	0	3.00	770.59	1.17	4.68	42.96	182.05	51.88	9.39	3.39	6.41	0.423
11	7.62	3.52	18.8	1,997	0	1.95	1012.6	1.33	6.69	50.16	171.26	47.75	31.5	2.51	13.91	0.621
12	7.61	2.95	16.5	1,674	0	1.62	866.07	0.41	4.98	15.60	112.44	33.34	47.36	22.93	6.2	0.537
13	6.87	3.20	15.9	1,126	0	2.78	526.75	2.11	5.10	32.81	76.97	27.01	20.97	32.65	3.83	0.425
14	7.47	3.70	16.7	1,008	0	1.05	534.20	1.49	4.60	11.34	104.89	31.56	8.33	4.30	5.44	0.447
15	7.25	5.86	16.7	842	22.2	1.50	452.75	5.25	3.29	11.54	100.01	29.74	0.18	0.22	3.97	0.386
19	9.39	7.51	15.7	442	321.1	0.97	18.12	14.72	0.88	1.21	67.85	20.99	0.05	0.03	0.01	0.326
20	3.48	7.09	16.4	740	318.7	26.51	126.26	39.9	8.60	15.15	93.18	23.77	0.01	0.01	0.02	0.542
22	3.30	7.19	17.1	373	212.5	4.10	31.05	9.80	1.89	5.76	58.71	16.93	0.05	0.02	bd	0.132
24	10.9	8.44	19.9	508	141.0	2.26	207.12	5.09	2.46	8.09	71.82	20.28	0.04	0.04	0.01	0.263
25	8.59	5.06	16.4	783	30.9	3.97	385.08	3.04	3.33	26.67	89.90	22.73	2.88	13.11	3.44	0.356
26	8.29	5.08	14.8	629	22.2	1.98	307.87	2.83	3.65	15.61	78.05	22.99	2.75	1.94	1.57	1.258
27	8.96	3.43	13.2	1,280	0	2.73	440.40	2.76	2.36	24.57	100.55	33.75	19.36	5.78	8.82	0.475

Table 2 continued

Sample no.	DO	pH	T	EC	HCO_3	Cl	SO_4	NO_3	K	Na	Ca	Mg	Al	Fe	Mn	As
28	7.77	3.10	14.9	2,230	0	3.22	777.19	3.23	5.04	57.71	141.78	7.05	4.70	6.55	13.63	0.611
30	7.63	3.30	15.7	1,632	0	3.53	529.32	3.87	4.65	85.72	131.17	41.14	0.03	0.10	5.52	0.855
31	7.79	3.33	17.3	1,391	0	3.40	998.00	3.66	2.64	25.34	100.03	31.8	23.66	131.81	9.78	0.511
32	8.45	5.22	15.2	1,039	21.0	2.25	633.16	1.45	2.94	26.26	118.52	38.44	18.98	15.36	7.45	0.354
33	7.64	3.30	18.3	1,295	0	3.50	620.85	7.92	3.00	26.42	102.05	31.90	1.29	4.77	2.61	0.495
38	6.79	5.40	22.1	808	49.2	2.08	597.25	1.81	3.37	17.25	101.14	24.50	18.24	12.07	7.23	1.413
39	9.53	3.56	13.7	983	0	1.96	503.06	1.78	2.87	18.42	96.60	26.28	0.55	2.85	2.33	0.424
41	8.50	3.28	17.5	1,138	0	1.60	569.45	2.64	2.76	17.04	87.67	27.04	9.46	7.32	3.49	0.400
42	6.26	6.54	17.9	831	30.6	1.84	448.63	1.66	3.13	23.17	102.35	24.63	0.02	1.00	2.15	0.320
43	3.25	7.44	24.3	667	163.2	1.99	289.06	2.19	2.82	10.98	82.58	26.91	0.05	0.02	0.41	0.749
44	6.59	3.31	29.4	952	0	1.20	472.68	1.80	2.79	7.42	93.72	26.10	12.59	27.02	4.56	0.454
46	6.13	7.15	29.3	454	49.8	1.15	221.68	2.21	1.96	5.22	62.24	14.68	0.04	0.02	0.91	0.244
48	7.57	2.97	24.9	1,216	0	1.19	533.52	0.79	2.74	5.64	93.69	24.59	3.83	2.65	2.25	0.465
49	6.55	4.36	22.7	829	0	1.44	466.01	2.93	2.71	5.68	96.06	27.61	6.73	8.30	3.26	1.152
50	9.74	8.16	16.2	463	192.1	2.03	130.12	3.70	1.64	5.22	62.51	18.27	0.01	0.02	bd	0.070
51	7.24	7.88	17.8	613	224.5	1.44	106.24	3.76	2.72	10.59	80.48	19.98	0.02	0.02	bd	0.115
52	7.51	7.74	22.4	762	313.9	27.76	170.52	14.87	11.87	29.32	79.87	24.89	0.04	0.02	0.06	0.522
53	10.25	7.60	17.9	483	192.7	1.82	141.40	5.81	1.62	4.36	67.97	15.63	0.03	0.01	0.01	0.067
54	9.65	7.94	18.6	540	227.5	6.56	148.24	4.66	3.56	9.57	70.36	17.84	0.02	0.02	0.03	0.250
55	8.60	7.90	19.5	530	217.3	6.78	149.65	7.84	3.61	9.37	70.02	18.25	0.02	0.01	0.03	0.255
56	7.64	7.90	19.7	526	240.7	6.04	138.92	7.50	3.30	8.32	68.91	18.62	0.02	0.01	0.01	0.674
57	9.12	7.99	18.8	525	226.3	5.74	143.34	4.47	3.19	7.84	68.32	18.94	0.02	0.01	bd	0.346
58	12.10	8.34	20.6	496	214.9	6.04	148.35	6.22	3.10	7.34	63.87	19.13	0.02	0.01	bd	0.957
59	7.48	8.18	22.1	507	201.1	5.61	157.26	7.37	3.47	7.85	69.68	19.91	0.06	0.07	0.02	0.337
Unaffected waters																
5	7.89	8.11	17.5	285	182.5	1.12	10.52	4.14	1.92	5.87	56.80	4.65	2.45	0.09	1.91	0.641
16	2.64	6.90	17.9	714	308.5	2.21	158.26	3.86	1.77	6.80	97.36	19.99	0.02	0.05	bd	0.401
17	3.67	7.15	16.4	601	468.2	5.49	37.80	19.37	2.26	3.68	73.77	28.91	bd	0.02	0.01	0.458
18	3.61	7.16	17.9	503	306.1	1.71	103.89	8.30	1.59	4.98	75.15	15.67	0.01	0.01	bd	0.287
21	5.34	7.04	14.6	125	129.9	0.52	11.78	2.72	0.87	5.27	27.14	3.59	0.01	0.02	bd	0.075
23	8.90	8.21	18.7	262	171.1	1.65	16.43	6.56	1.18	4.77	50.19	8.68	0.03	0.02	bd	0.074
29	8.17	7.08	16.0	604	51.6	1.62	258.96	3.12	1.60	8.47	74.61	26.13	0.06	0.01	bd	0.080
34	8.45	6.77	17.4	305	33.6	1.76	175.70	2.97	1.58	3.34	47.65	11.55	0.01	0.01	0.03	0.090
35	7.25	7.50	15.7	169	128.7	0.95	19.16	5.28	0.92	2.29	34.11	5.00	0.01	bd	0.0003	0.048
36	6.91	7.97	20.1	192	135.6	1.80	12.92	0.13	1.90	6.11	39.85	3.85	0.03	0.02	0.0025	0.073
37	8.33	8.24	22.5	261	42.0	1.49	126.21	2.07	1.72	8.19	42.63	7.45	0.16	0.01	0.01	0.059
40	8.24	7.89	14.9	158	121.2	0.33	2.44	5.28	0.83	2.12	35.95	2.48	0.06	0.04	0.01	0.043
45	7.54	8.31	27.7	199	130.8	1.11	26.69	2.30	1.36	4.59	37.05	4.93	0.01	0.02	bd	0.058
47	9.21	8.67	20.6	193	118.8	1.13	25.08	1.04	1.07	4.30	34.94	4.77	0.05	0.01	0.01	0.063

Ion concentrations in milligrams per liter, except for As (μg/L); temperature in °C; pH in pH units; *EC*, electrical conductivity in μS/cm at 25°C; *bd*, below detection limits

References

Accornero M, Marini L, Ottonello G, Vetuschi Zuccolini M (2005) The fate of major constituents and chromium and other trace elements when acid waters from the derelict Libiola mine (Italy) are mixed with stream waters. Appl Geochem 20:1368–1390

Allen SK, Allen JM, Lucas S (1996) Concentrations of contaminants in surface water samples collected in west-central Indiana impacted by acidic mine drainage. Environ Geol 27:34–37

Benjaminn MM (1983) Adsorption and surface precipitation of metals of amorphous iron oxyhydroxide. Environ Sci Technol 17:686–692

Berger AC, Bethke CM, Krumhansl JL (2000) A process model of natural attenuation in drainage from a historic mining district. Appl Geochem 15:655–666

Bigham JM (1994) Mineralogy of ochre deposits formed by sulfide oxidation. In: Jambor JL, Blowes DW (eds) Short course handbook on environmental geochemistry of sulfide mine-wastes. Mineralogical Association of Canada, Toronto, ON, Canada, pp 103–132

Bigham JM, Schwertmann U, Carlson L, Murad E (1990) A poorly crystallized oxyhydroxysulfate of iron formed by bacterial oxidation of Fe(II) in acid mine waters. Geochim Cosmochim Acta 54:2743–2758

Bigham JM, Schwertmann U, Traina SJ, Winland RL, Wolf M (1996) Schwertmannite and the chemical modeling of iron in acid sulfate waters. Geochim Cosmochim Acta 60:2111–2121

Black A, Craw D (2001) Arsenic, copper and zinc occurrence at the Wangaloa coal mine, southeast Otago, New Zealand. Int J Coal Geol 45:181–193

Bodénan F, Baranger P, Piantone P, Lassin A, Azaroual M, Gaucher E, Braibant G (2004) Arsenic behaviour in gold-ore mill tailings, Massif Central, France: hydrogeochemical study and investigation of in situ redox signatures. Appl Geochem 19:1785–1800

Bowell RJ, Bruce I (1995) Geochemistry of iron ochres and mine waters from Levant mine, Cornwall. Appl Geochim 10:237–250

Devasahayam S (2006) Chemistry of acid production in black coal mine washery wastes. Int J Miner Process 79:1–8

Ding ZH, Zheng BS, Zhang J, Belkin HE, Finkelmam RE, Zhao FH (1999) Pilot study on model of occurrence of arsenic in high as coals from southwest Guizhou provience. Sci Chin (Series D) 29(5):421–425

Ding ZH, Zheng BS, Finkelman RB, Belkin HE, Chen CG, Zhou DX, Zhou YS (2000) Distribution of high arsenic coals from southwest Guizhou Province. Geochimical 29(5):493–494

Evangelou VP (1995) Pyrite oxidation and its control. CRC Press, Boca Raton, FL, p 293

Faure G (1998) Principles and applications of geochemistry. Prentice Hall, Upper Saddle River, NJ

Foos A (1997) Geochemical modeling of coal mine drainage, Summit county, Ohio. Environ Geol 31(3/4):205–210

Fukushi K, Sasaki M, Sato T, Yanase N, Amano H, Ikeda H (2003) A natural attenuation of arsenic in drainage from an abandoned arsenic mine dump. Appl Geochem 18:1267–1278

Garcia-Sanchez A, Alvarez-Ayuso E, Rodriguez F (2002) Sorption of As(V) by some oxyhydroxides and clays minerals. Application to its immobilization in two polluted mining soils. Clay Miner 37:187–194

Han GL, Liu CQ (2004) Water geochemistry controlled by carbonate dissolution: a study of the river waters draining karst-dominated terrain, Guizhou Province, China. Chem Geol 204:1–21

Holmström H, Ljungberg J, Öhlander B (1999) Role of carbonates in mitigation of metal release from mining waste. Evidence from humidity cells tests. Environ Geol 37(4):267–280

Johnson CA, Thornton I (1987) Hydrological and chemical factors controlling the concentrations of Fe, Cu, Zn and As in a river system contaminated by acid mine drainage. Water Res Bull 21:359–365

Johnson RH, Blowes DW, Robertson WD, Jambor JL (2000) The hydrogeochemistry of the nickel rim mine tailings impoundment, Sudbury, Ontario. J Contam Hydrol 41:49–80

Kim JY, Chon HT (2001) Pollution of a water course impacted by acid mine drainage in the Imgok creek of the Gangreung coal field, Korea. Appl Geochem 16:1387–1396

Lee G, Bigham JM, Faur G (2002) Removal of trace metals by coprecipitation with Fe, Al and Mn from natural waters contaminated with acid mine drainage in the Ducktown Mining District, Tennessee. Appl Geochem 17:569–581

Li DH, Chen K, Deng T, Cheng FP, Yang J (2003) Content and corredation of arsenic in coal of southwest China area. Coal Geol Chin 31(4):419–423

Ljungberg J, Lindvall M, Holmström H, Öhlander B (1997) Geochemical field study of flooded mine tailings at Stekenjokk, northern Sweden. In: Proc 4th Int Conf on Acid Rock Drainage, Vancouver, BC, 31 May–6 June 1997, 3:1401–1418

Lowson RT (1982) Aqueous oxidation of pyrite by molecular oxygen. Chem Rev 82:461–497

Mayo AL, Petersenb EC, Kravitsc C (2000) Chemical evolution of coal mine drainage in a non-acid producing environment, Wasatch Plateau, Utah, USA. J Hydrol 236:1–16

Nordstrom DK (1982) The effect of sulfate on aluminum concentrations in natural waters: somestability relations in the system Al_2O_3-SO_3-H_2O at 298 K. Geochim Cosmochim Acta 46:681–692

Nordstrom DK, Ball JW (1986) The geochemical behavior of aluminum in acidified surface waters. Science 232:54–56

Parkhurst DL (1995) User's guide to PHREEQC: a computer program for speciation, reaction-path, advective transport and inverse geochemical calculations (Water Resources Investigations Report). US Geological Survey, Reston, VA

Parkhurst DL, Appelo CAJ (1999) User's guide to PHREEQC(version 2)—a computer program for speciation, batch-reaction, one-dimensional transport, and inverse geochemical calculations (Water Resources Investigations Report 99-4259). US Geological Survey, Reston, VA

Raven KP, Jain A, Loeppert RH (1998) Arsenite and arsenate adsorption on ferrihydrite: kinetics, equilibrium, and adsorption envelopes. Environ Sci Technol 32:344–349

Sánchez-Espańa FJ, López Pamo E, Santofimia Pastor E, Reyes Andrés J, Martín Rubí JA (2006) The removal of dissolved metals by hydroxysulphate precipitates during oxidation and neutralization of acid mine waters, Iberian pyrite belt. Aquatic Geochem 12:269–298

Schuring J, Kolling M, Schulz HD (1997) The potential formation of acid mine drainage in pyrite bearing hard-coal tailings under water-saturated conditions: an experimental approach. Environ Geol 31(1/2):59–65

Stumm W, Sulzberger B (1992) The cycling of iron in natural environments: considerations based on laboratory studies of heterogeneous redox processes. Geochim Cosmochim Acta 56:3233–3257

Tiwary RK (2001) Environmental impact of coal mining on water regime and its management. Water Air Soil Pollut 132:185–199

Williams DJ, Bigham JM, Cravotta CA, Traina SJ, Anderson JE, Lyon JG (2002) Assessing mine drainage pH from the color and spectral reflectance of chemical precipitates. Appl Geochem 17:1273–1286

Xie F, He JL, Tan H, Deng QJ, Song CR, Chen AN, Ji YB (2006) Determination of cadmium, arsenic and mercury in soil with nitric acid digestion technique. Chin J Soil Sci 37:340–342

Yu J, Heo B, Choi I, Cho J, Chang H (1999) Apparent solubilities of schwertmannite and ferrihydrite in natural stream waters polluted by mine drainage. Geochim Cosmochim Acta 63:3407–3416

Yu JY (1996) Pollution of Osheepcheon Creek by abandoned coal mine drainage in Dogyae area, eastern part of Samcheok coal field, Kangwon-Do, Korea. Environ Geol 27:286–299

Zhao FH, Ren DY, Peng SP, Wang YQ, Zhang JY, Ding ZH, Cong ZY (2003) The modes of occurrence of arsenic in coal. Adv Earth Sci 18(2):214–220

Zheng BS, Ding ZH, Huang RG, Zhu JM, Yu XY, Wang AM, Zhou DX, Mao DJ, Su HC (1999) Issues of health and disease relating to coal use in southwestern China. Int J Coal Geol 40:119–132

Zhou DX, Liu DN, Zhu SL, Zhou CL (1993) Investigation of chronic arsenic poisoning caused by high arsenic coal pollution. Chin J Prev Med 27:147–150